Lithium electrodeposition for energy storage: filling the gap between theory and experiment

(article starts on next page)

Perspective

Lithium electrodeposition for energy storage: filling the gap between theory and experiment

Shizhao Xiong [a], [*], Leif Nyholm [b], [**], Aleksandar Matic [a], Chao Zhang [b], [***]

[a] *Department of Physics, Chalmers University of Technology, Göteborg SE 412 96, Sweden*
[b] *Department of Chemistry-Ångström Laboratory, Uppsala University, Lägerhyddsvägen 1, P. O. Box 538, 75121 Uppsala, Sweden*

ARTICLE INFO

ABSTRACT

Lithium (Li) metal has been considered a promising anode material for high-energy-density rechargeable batteries, but its utilization is impeded by the nonuniform electrodeposition during the charging process which leads to poor cycling life and safety concerns. Thus, understanding the electrodeposition mechanism of Li-metal anode is of great importance to develop practical engineering strategies for rechargeable Li-metal batteries. The electrodeposition of Li is controlled by both thermodynamic and kinetic factors, such as the solvation free energy of Li-ions, the Li nucleation, the surface diffusion of Li atom, and the strength of the interaction between Li-ion and the electrolyte anion. The scale of the whole process from the Li-ion reduction to the growth of a Li nucleus goes from sub-nanometer up to a few micrometers, which poses an outstanding challenge to both experiments and simulation. In this perspective, we discuss the top-down, the bottom-up, and the middle-way approaches to this challenge and the possible synergies between them.

1. Introduction

Advanced battery technologies are playing a critical role in the transition to a climate-neutral society by enabling electrification of transport, as well as being intermittent electricity sources for renewable energies, such as solar and wind power [1]. While the state-of-the-art lithium-ion batteries (LIB) can deliver gravimetric energy densities up to 300 Wh/kg by materials optimization and cell design, this value is approaching its limit [2]. To satisfy applications inherently requiring higher energy densities, like electrification of aircraft, the introduction of entirely new technologies or chemistries for next-generation secondary battery systems is needed, e.g., solid-state batteries, lithium-air (Li-air) batteries, or lithium-sulfur (Li−S) batteries [3]. One of the keys to realizing these technologies is the utilization of lithium (Li) anodes to match the very high capacity on the cathode side and achieve the goal of high energy density [4].

The primary challenge in the utilization of Li anode is a nonuniform deposition of metal during the charging process and a thermodynamically unstable interface toward the electrolyte. The deposition of Li metal from the electrolyte commonly results in a dendritic and porous structure with large surface area, rather than the desired dense and bulk metallic electrode, resulting in low Coulombic efficiency and decaying electrochemical performance and potential safety issues [5]. The formation of Li dendrites is strongly related to the nature of the reduction process of Li-ions, the nucleation of Li atoms at the substrate, and mass transfer kinetics at the interface between the Li anode and electrolyte. The interface of the Li anode is also thermodynamically unstable toward common electrolytes, and a passivation layer will spontaneously be created by the reaction between the electrolyte and Li [6]. The formation of this surface layer, the solid electrolyte interphase (SEI), at the initial state as well as during cycling will consume the active Li metal and electrolyte, shortening the battery cycle life. In addition, dendrites and porous structures covered with the SEI risk becoming electronically separated from the bulk metal during cycling. This leads to an inactive mass being accumulated at the interface and induces high interfacial resistance and lower Coulombic efficiency, both of which will lead to the capacity fading of batteries [5,7,8]. Therefore, understanding the nucleation, the morphology formation, and the SEI evolution on Li anode, particularly for the electrodeposition

---

* Corresponding author.
** Corresponding author.
*** Corresponding author.
    E-mail addresses: shizhao.xiong@chalmers.se (S. Xiong), leif.nyholm@kemi.uu. se (L. Nyholm), chao.zhang@kemi.uu.se (C. Zhang).

process, is the key to design advanced engineering strategies for the unitization of Li anode in high-energy-density batteries [9].

To capture the interface evolution and SEI structures on Li anodes, various characterization methods have been developed, including high-resolution cryo-electron microscopy, operando X-ray tomography, optical microscopy, and in situ X-ray photoelectron spectroscopy [10]. These techniques can monitor the interface structure of Li during the electrodeposition process, covering the initial states (10−100 nm) to the final morphology (1−10 μm). However, each diagnostic tool has certain limitations, hindering the understanding of the Li interface through the fundamental theory or under various conditions. Numerical simulation methods are also introduced to provide a theoretical understanding of specific steps or scale for the electrodeposition behavior of Li. For instance, first-principles simulations based on the density functional theory (DFT) have been used to explore the decomposition of gas molecules on Li for stabilizing Li anodes by surface treatment [11]. Moreover, molecular dynamics (MD) simulations have been employed to understand the growth mechanism during the Li electrodeposition at the atomic scale [12]. Finite element method based on a thermodynamically consistent theory is also a powerful tool to simulate the electro-chemo-mechanics of Li growth regarding the impact of mass transport, electrodeposition, and deformation at the interface [13].

Despite remarkable results obtained by simulation methods, the electrochemical conditions used in simulations are usually not representative enough for the real situation in electrochemical cells during experiments, not to mention the risk of overlooking alternative mechanisms. Therefore, the simulation results may show a similar trend as in the experiment, but they may not be correct for the right reasons. In this perspective, we try to bridge the fundamentals and the typical practice in the Li electrodeposition in an attempt to seek synergy between theory and experiments. Therefore, our strategy is not to exhaustive review the topic but rather to bring up points that are insufficiently discussed in the literature with a clear focus on lithium-metal battery systems containing liquid electrolytes. Recent progress on both atomistic simulation and phase-field modeling of the space-charge layer as well as Li dendrite formation in solid electrolytes can be found elsewhere [14−17].

2. Thermodynamics and interface

The reduction potential of Li^+ in aqueous solution is -3.04 V versus the standard hydrogen electrode (SHE). Since Li metal strongly reacts with water, this value is actually experimentally determined with respect to the lithium amalgam [18]. Nevertheless, it would be instructive to describe how one can obtain the standard reduction potential of Li^+ through the so-called thermodynamic cycle.

As illustrated in Fig. 1a, the overall reaction of Li^+ reduction can be calculated based on the following three steps:

$$Li\,(s) \rightarrow Li\,(g)\,, \tag{1}$$

$$Li\,(g) \rightarrow Li^+\,(g) + e^-\,, \tag{2}$$

$$Li^+\,(g) \rightarrow Li^+\,(sol)\,. \tag{3}$$

The reverse of $(1) + (2) + (3)$ leads to the Li^+ reduction reaction in aqueous solution. The corresponding energic changes accompanying these three processes are the heat of sublimation ΔH_{sub}, the ionization potential (IP), and the solvation free energy (ΔG_{sol}). Note that both ΔH_{sub} and IP are positive, whereas ΔG_{sol} is negative. Results of such calculations are present in Table 1, where values for
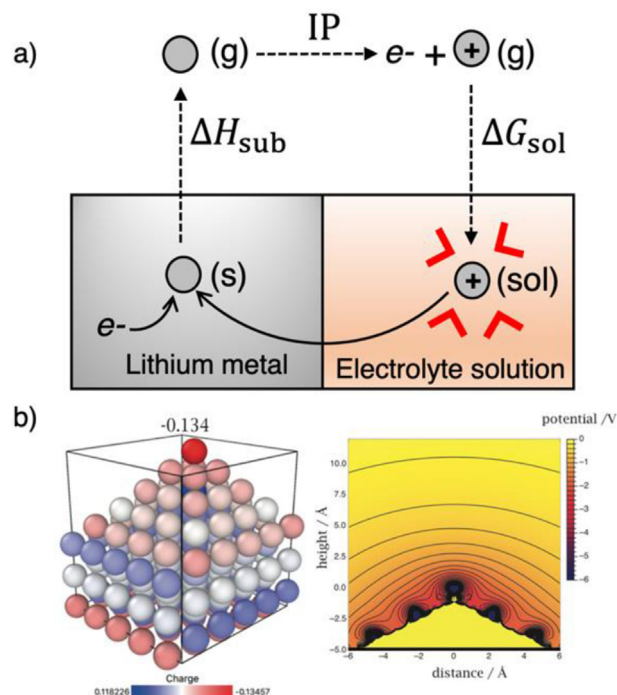

Fig. 1. (a) Thermodynamic cycle for Li electrodeposition reaction; (b) the charge distribution of a model Li pyramid at -3.04 versus SHE. Adapted from Ref. [19] under the terms of CC-BY license (Copyright 2021 Authors).

other monovalent metal ions such as Na^+, K^+, Ag^+ are also given, in addition to the case of Li^+.

The significance of Table 1 lies in the fact that the standard reduction potential of Li^+ depends on the type of solvent. By decreasing the solvation free energy, the reduction potential of Li^+ can become more positive. Further, it suggests that counterions would play a significant role, where the ion-pairing and the ion correlation can significantly change the activity coefficient and the concentration of free Li^+. It is worth mentioning that ΔH_{sub}, IP, and ΔG_{sol} are all accessible thermodynamic quantities from first-principles simulations [24−26].

Li electrodeposition obviously involves the interface between the lithium metal and the electrolyte solution, as depicted in Fig. 1a. However, the interface does not show up in the thermodynamic cycle discussed so far. This means that one could rewrite the Li^+ reduction reaction in order to reveal the role of the interface, as shown below:

$$Li^+\,(sol) + * \rightarrow Li^+ *\,, \tag{4}$$

$$Li^+ * + e^- \rightarrow Li^*\,(s)\,, \tag{5}$$

$$Li^*(s) \rightarrow Li\,(s)\,. \tag{6}$$

Table 1
Reduction potential for Li^+ together with other common monovalent ions. $E^0_{pred} = ((\Delta H_{sub} + IP + \Delta G_{sol})/e - 4.44$ V. Values of ΔH_{sub} and ΔG_{sol} are taken from Refs. [20,21], respectively, while both IP and E^0_{ref} come from Ref. [22]. The recommended value for the absolute SHE is 4.44V [23].

	Li^+	Na^+	K^+	Ag^+
ΔH_{sub} (eV)	1.65	1.11	0.92	2.95
IP (eV)	5.39	5.14	4.34	7.57
ΔG_{sol} (eV)	−5.48	−4.39	−3.65	−5.07
E^0_{pred} (V)	−2.88	−2.58	−2.82	1.01
E^0_{ref} (V)	−3.04	−2.71	−2.93	0.80

where asterisk * indicates the surface site, which is commonly used in surface science.

The importance of reactions (4) − (6) is that it follows the sequential steps of Li electrodeposition, i.e., the diffusion and the adsorption of Li$^+$ on the surface, the charge-transfer reaction at the surface, and the nucleation to form the Li metal. Since the charge-transfer reaction is normally considered [27] to be the fastest among these three, reactions (4) and (6) are therefore the rate-limiting steps composed of multiple elementary reactions. Here, we focus on reaction (4).

As recently pointed out by Santos and Schmickler [19], the standard reduction potential of Li$^+$ (-3.04 versus SHE) is lower than the potential of zero charge (PZC) of lithium metal (-1.91 versus SHE). A similar conclusion was drawn previously based on the first-principles calculation [28]. This means that the lithium electrode will bear a negative charge at the nominal deposition potential. Looking at the reaction (5), it is clear that the electrostatic interaction between the negatively charged lithium metal and the lithium-ion will drive the reaction. More interestingly, the negative charge will not be distributed uniformly when the surface of the lithium metal is rugged rather than ideally flat. As illustrated in Fig. 1b, the model electrode with a pyramid shape shows that the negative charge is localized around the tip of the pyramid. This has a strong indication that the Li deposition does not happen uniformly, and that dendrite growth is inevitable. It further suggests that the geometry, the roughness, and the defects at the lithium metal surface are crucial for the initial step during the Li deposition.

To close this section, it is worth noting that the solvent, the counterion, and the interfacial electric field have an even more critical role in influencing the kinetics of the Li electrodeposition yielding various overpotentials [29]. In addition, the interface also plays a crucial role in reaction (6) which involves the surface diffusion [30] and the nucleation mechanism, as discussed in the next section.

3. 2D versus 3D lithium nucleation and growth on lithium and copper electrodes

As already indicated in the introduction, lithium deposition in conventional electrolytes, e.g., 1 M LiPF$_6$ in EC:DEC (1:1), typically results in the formation of deposits composed of porous lithium, lithium dendrites, and dead lithium [5,31]. This problem is typically addressed using electrolyte additives or functionalized layers on the electrode to stabilize the SEI layer and subsequently decrease the risk of lithium dendrite formation. Very few studies have, so far, focused on obtaining 2D rather than 3D nucleation and growth by electrochemically modifying the lithium nucleation conditions. This is surprising as it is well known [32,33] that the number of nuclei formed on the electrode depends exponentially on the employed overpotential. At low overpotentials, only a few nuclei would be expected to form on the (most active deposition sites) of the lithium electrode, favoring the generation of a 3D deposit (i.e., porous lithium, dead lithium, and dendrites). This becomes a major problem when using a lithium electrode immersed in electrolytes containing 1 M lithium salt since the lithium electrode then would act essentially as a nonpolarizable electrode. In conventional electrolytes (as well as in solid electrolytes), it should, therefore, be very difficult to reach the overpotentials needed to ensure 2D nucleation and growth on lithium metal electrodes. This is in excellent agreement with the experimental findings for liquid electrolytes [5,31].

The key to obtaining a homogeneous distribution of lithium nuclei on the entire electrode surface is consequently the ability to apply a sufficiently large overpotential to the electrode. The question is then if 2D nucleation and growth can be obtained using approaches based on electrolyte additives or functional coatings on the lithium electrode? This seems unlikely, at least when using a lithium salt concentration of 1 M. While the formation of lithium complexes with ligands in the electrolyte can increase the overpotential by decreasing the free Li$^+$ concentration in the electrolyte, the effect is most likely too small to give rise to the large overpotentials needed to ensure 2D nucleation and growth. However, it has been demonstrated [34] that 2D nucleation and growth can be obtained by decreasing the concentration of the lithium salt in the electrolyte from 1 M to 20 mM. This allows a very short (e.g., 10 ms long) nucleation pulse to be used to generate small nuclei on the entire electrode surface. Here, it is very important that the lithium nuclei are formed simultaneously, i.e., that the nucleation and growth are instantaneous rather than progressive. After the nucleation step, the lithium nuclei are then allowed to grow at a lower overpotential where no new nuclei are formed, e.g., using conventional constant-current deposition conditions. In this approach to realize 2D lithium deposition and growth, schematically described in Fig. 2, a supporting electrolyte can also be used to ensure that the conductivity of the electrolyte remains essentially unchanged. With a supporting electrolyte, the migration of Li$^+$ is also essentially eliminated which should decrease the risk of the formation of dendrites, as schematically shown in Fig. 2. The fact that the mass transport of Li$^+$ to the electrode then becomes diffusion controlled further ensures a homogeneous lithium deposition. While the approach, described in Fig. 2, is promising, more work is clearly needed to further evaluate this approach.

In addition to the large interest in the deposition of lithium-on-lithium electrodes, there is also a significant interest in the deposition of lithium on copper electrodes [35,36]. It has, for example, been proposed that lithium may be deposited directly on copper current collectors or porous copper electrodes with large surface areas [36,37]. As will be described below, the attainment of 2D deposition of lithium on copper electrodes may, however, be even more difficult to obtain than that on lithium electrodes. One additional complication is that small lithium nuclei formed on a copper electrode will diffuse into the copper electrode [38] as lithium and copper form a solid solution. Since the lithium nuclei are less stable on a copper electrode (than on a lithium electrode), it should be more difficult to obtain 2D nucleation and growth on a copper electrode. Another complication is that the lithium deposition potential will vary during the deposition due to underpotential deposition of lithium on copper. Since the lithium activity in the pristine copper electrode should be much lower than unity, the lithium deposition potential will decrease when the activity of lithium in the copper electrode increases (this is immediately apparent from the Nernst equation). Here, it should be recalled that the standard potential for the Li$^+$ + e$^-$ = Li reaction only is valid for an electrolyte containing 1 M Li$^+$ and a lithium electrode with unit lithium activity. Studies of the deposition of lithium on copper electrodes are also complicated by the fact that the copper electrode typically has an oxide layer (e.g., Cu$_2$O or CuO) on its surface. This oxide layer then undergoes a conversion reaction (e.g., Cu$_2$O + 2 e$^-$ + 2 Li$^+$ = 2 Cu + Li$_2$O) yielding a matrix composed of copper nanoparticles and Li$_2$O on the surface of the copper electrode. As a result, the surface of the obtained copper electrode should be significantly less well defined than that of a lithium electrode. Finally, it should be mentioned that lithium deposition on porous copper substrates is unlikely to yield competitive lithium metal electrodes mainly as their capacities typically will be too low. This becomes particularly evident when also considering the weight of the electrolyte present in the porous electrode.

To realize stable lithium metal electrodes, more attention should be paid to the nucleation and growth of lithium-on-lithium electrodes. As mentioned above, it will be very difficult to avoid the
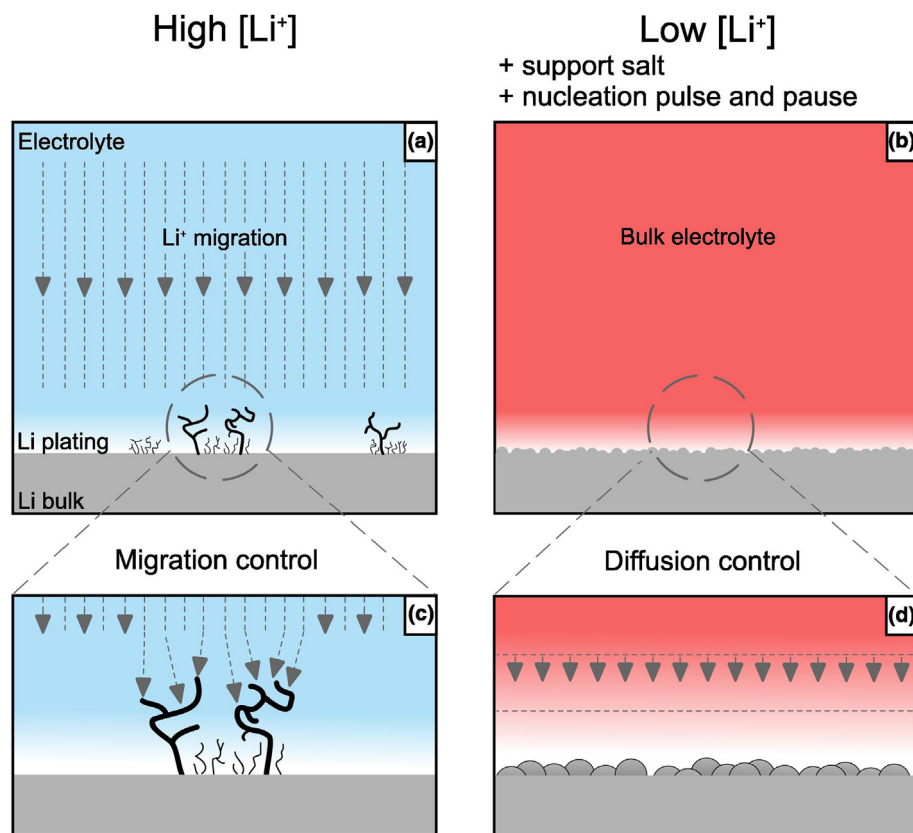
Fig. 2. Schematic illustrations of the lithium-on-lithium deposition conditions in electrolytes containing a conventional (A and C) and significantly lower (B and D) lithium salt concentration, respectively. High [Li$^+$] images represent the conditions during conventional lithium deposition in 1.0 M LiPF$_6$, whereas a nucleation pulse and pause were assumed to be used together with the Low [Li$^+$] electrolyte. Lower figures (c and d) depict magnifications of the regions indicated in the upper figures. Note the larger number of nuclei and hence the more two-dimensional-like deposition in the Low [Li$^+$] electrolyte [34].

formation of porous lithium, dead lithium, and dendrites if 2D deposition and growth cannot be realized. It is, therefore, very unlikely that stable lithium metal electrodes can be realized by merely using approaches based on the inclusion of additives in the electrolyte or functionalized layers on the surfaces of electrodes. Given that 3D lithium deposition is very likely to be observed under conventional experimental conditions, one important question is how the morphologies and microstructures of the lithium deposits can be controlled. As will be discussed in the next section, phase-field modeling can be used to shed light on this topic.

4. Growth of Li nucleus to microstructures

The morphology of electrodeposited Li is highly dependent on the electrochemical environment which depends on the nano-structure and chemistry of the electrolyte, the tortuosity of the substrate, the properties of the SEI, as well as the operation conditions [39]. Owing to the complexity of the electrochemical process, the electrodeposited Li has been reported to have various morphologies, such as needle-like [40], mossy-like [39], sheet-like [40], or pillar-like [41], depending on the conditions employed, including the electrolyte formulation, applied current density, temperature, and stack pressure.

From a fundamental electrochemical point of view, the final morphology of the deposit is mainly determined by the mass transfer of Li-ions in the liquid electrolyte as well as the stability of the ion-conductive SEI layer on the Li anode [42]. A strong concentration gradient induced by the low Li-ion mass transfer rate is believed to lead to the formation of Li dendrites. Moreover, the thin

SEI layer may break when its mechanical strength is not enough to adapt to the fluctuating electrode surface. This will trigger side reactions between the freshly exposed Li and electrolyte, irreversibly consuming both active Li and electrolyte. Therefore, it is very important to understand the dynamic correlation between the electrodeposition of Li and multi-physics fields during the Li growth process.
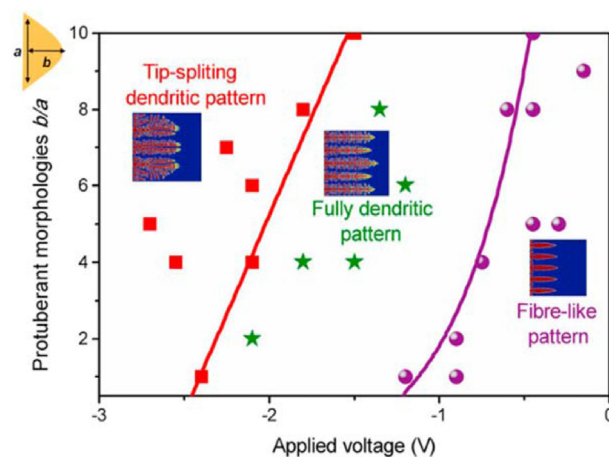

Fig. 3. Phase-field modeling results reveal the correlation of the final pattern of the electrodeposited Li and the applied electrostatic potential in the electrodeposition system, as well as the initial morphology. Reproduced from Ref. [43]. Copyright (2015) Elsevier.
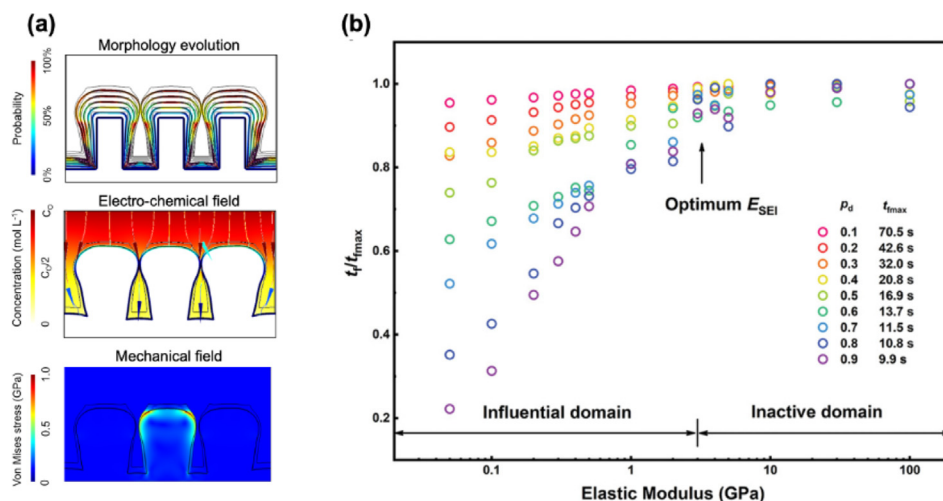
Fig. 4. (a) Electro-chemo-mechanical modeling of electrodeposited Li covered by a SEI layer. Reproduced from Ref. [46]. Copyright (2022) The Authors. Published by WILEY-VCH under a CC-BY license. (b) The relationship between the failure time and the elastic modulus of the SEI layer on a Li-metal anode. Reproduced from Ref. [47]. Copyright (2020) WILEY-VCH.

A thermodynamically consistent phase-field model was built by Liu et al. to study the influence of the electrochemical overpotential, which is determined by the electrostatic potential and the lithium-ion concentration, on the formation of patterns of Li dendrites [43]. In this model, the nonlinear evolution of the phase-field model is treated with an electrochemical overpotential. Therefore, the electrochemical kinetics is captured by monitoring the change of mass transfer of Li-ions and the local electrostatic potential. As shown in Fig. 3, it is found that the final morphology of the deposited Li is strongly dependent on the applied voltage and the initial morphology of the electrode surface. A phase-like diagram was constructed to identify regions yielding fiber-like Li, intact dendrites, as well as tip-splitting dendrites with two boundary lines. The x-axis of the diagram is the applied voltage while the y-axis is the size ratio (b/a) of the protuberance that is representative of the initial morphology of the Li. The transition from fiber-like Li to intact dendrites and tip-splitting dendrites will be seen when increasing the applied voltage or when making the initial morphology of the electrode flatter. It is worth noting that the thermodynamic aspect of the potential dependence may also be taken into account with Pourbaix-type diagrams, using a computational lithium electrode (CLiE) approach [44,45].

Apart from the electrochemical conditions, the mechanical stability of the SEI layer is also assumed to be critical for the electrodeposition of Li because the Li^+ ion transport through the SEI layer affects the kinetics of electrodeposition process and as mechanical damage of the SEI layer leads to side reactions. Quantitative electro-chemo-mechanical models have been built to understand the failure mechanism of the SEI layer and the influence of the properties of the SEI layer on the Li electrodeposition process [46,47]. In these models, the distribution of the Li-ion concentration, electric field, and the mechanical stress are directly visualized, as shown in Fig. 4a. The dynamic evolution of the physical fields and Li morphology are captured to study electrodeposition process which involves the reduction of Li-ions, changes in the stress at the interface, and mass transfer in the electrolyte. The results suggest that the structural uniformity of the SEI layer is the most significant parameter and that a high SEI ionic conductivity is beneficial to suppress stress at the interface, which is the primary cause of the rupture of the SEI layer. However, the modeling results also show that an extremely high Young's modulus of the SEI layer will suppress the electrodeposition rate of

Li without significantly improving the stability of the SEI layer (Fig. 4b). A moderate Young's modulus, about 3 GPa, is suggested as the optimum value to obtain a stable SEI layer on a Li-metal anode. Differing from previous directions, aimed at obtaining SEI layers with much higher mechanical strengths, the conclusions derived from the phase-field modeling present new insights into the Li electrode failure mechanism and the design of SEI layers. These new modeling directions are, therefore, promising in the development of advanced engineering strategies for practical applications of Li-metal batteries.

Although the phase-field modeling, based on electrochemical principles, is a powerful tool to investigate the morphological evolution of the Li deposited under various conditions, it is worth emphasizing that the electrochemical conditions used in the modeling cannot fully represent the real experimental conditions. Therefore, incorporating more experimental details into the model will significantly enhance the accuracy of modeling results and promote the development of phase-field modeling of electrochemical systems.

5. Conclusion and outlook

In this perspective, we return to the fundamentals of the deceivingly simple process of Li electrodeposition, and the three parts discussed represent three different approaches to the problem, namely, the bottom-up, the top-down, and the middle-way.

In the bottom-up approach, one tends to think (and compute) from the first-principles. This allows one problem to be tackled at a time and to single out factors that may otherwise be overlooked. Going from the thermodynamic cycle to the solvation free energy and showing the importance of the charge distribution in Li clusters are examples of this type of approach. The top-down approach, on the other hand, involves facing the full complexity seen within the experimental world. In this regard, the holistic view, as well as insights based on fundamental electrodeposition theory (e.g., the potential-controlled 2D nucleation and the underpotential deposition on the copper substrate), are shown to be valuable also for Li deposition. Finally, the middle-way approach, exemplified by the phase-field modeling method mentioned above, combines inputs from experiments with the physical laws emerging from the microscopic world. This allows one to do systematic studies under different electrochemical and mechanical conditions, which either

are too expensive to treat with first-principles simulations or difficult to address experimentally.

Nevertheless, there is no one-size-fits-all approach, and synergies are clearly needed in order to fill the gap between theory and experiment. In our view, this requires efforts considering at least two aspects: improved communication between researchers using different approaches and the incorporation of more realistic simulation conditions.

One way to think about first-principles simulation, phase-field modeling and experimental characterization is to consider these as different methods providing information at different levels. Therefore, parameters from the first-principles simulation and the experiments can be passed on to the phase-field modeling. For example, the solvation free energy computed from the first-principles simulation may be incorporated into the modeling of the surface tension in the phase-field modeling, while the morphology of the electrode determined from X-ray tomography can be used as a starting point when building an initial model. It is worth noting that the message-passing between different approaches is not a one-way street, for example, the constraints obtained from experiments (e.g., the composition or measurable constants) can be imposed in the first-principles simulation as well.

Another way to see the difference between theory and experiment is to realize that something simple in one approach can be rather challenging in the other or vice versa. For example, the surface defects, the site energy, the ligand complexation, and the ion-ion correlation that come naturally in first-principles simulation are not usually considered in the phase-field modeling because these factors are no longer simple functions of concentration and/ or electrostatic potential. Similarly, the experimental condition in the electrodeposition can switch between potentiostatic and galvanostatic, while the Dirichlet boundary condition (i.e., at a constant potential) is mostly applied in the phase-field modeling instead when solving the Li^+ diffusion equation and the electrostatic Poisson equation.

All in all, there is plenty of room where the bottom-up, the top-down, and the middle-way approaches can work together to improve our understanding of the fundamental process involved in the Li electrodeposition process and design new strategies for preventing/mitigating Li dendrite formation. Therefore, the seemingly large gap between theory and simulation is not really a challenge but an invitation.

CRediT (Contributor Roles Taxonomy) author statement

Shizhao Xiong: conceptualization, investigation, writing-original draft.

Leif Nyholm: conceptualization, investigation, writing-original draft, funding acquisition.

Aleksandar Matic: writing - review & editing, funding acquisition.

Chao Zhang: conceptualization, investigation, writing-original draft, funding acquisition.

Declaration of competing interest

The authors declare that they have no known competing financial interests or personal relationships that could have appeared to influence the work reported in this paper.

Acknowledgement

References

[1] V. Viswanathan, A.H. Epstein, Y.-M. Chiang, E. Takeuchi, M. Bradley, J. Langford, M. Winter, The challenges and opportunities of battery-powered flight, Nature 601 (2022) 519−525.

[2] B. Han, D. Xu, S.-S. Chi, D. He, Z. Zhang, L. Du, M. Gu, C. Wang, H. Meng, K. Xu, Z. Zheng, Y. Deng, 500 Wh kg−1 class Li metal battery enabled by a self-organized core−shell composite anode, Adv. Mater. 32 (2020) 2004793.

[3] C.P. Grey, D.S. Hall, Prospects for lithium-ion batteries and beyond—a 2030 vision, Nat. Commun. 11 (2020) 6279.

[4] Y.Y. Hu, R.X. Han, L. Mei, J.L. Liu, J.C. Sun, K. Yang, J.W. Zhao, Design principles of MOF-related materials for highly stable metal anodes in secondary metal-based batteries, Mater. Today Energy 19 (2021) 100608.

[5] K. Tang, J. Xiao, M. Long, J. Chen, H. Gao, H. Liu, G. Wang, Engineering a heteroatom-doped multidimensional carbon network for dendrite-free lithium metal anode, Mater. Today Energy 24 (2022) 100949.

[6] X. Shen, R. Zhang, P. Shi, X. Chen, Q. Zhang, How does external pressure shape Li dendrites in Li metal batteries? Adv. Energy Mater. 11 (2021) 2003416.

[7] J. Tan, M. Ye, J. Shen, Tailoring uniform and ordered grain boundaries in the solid electrolyte interphase for dendrite-free lithium metal batteries, Mater. Today Energy 22 (2021) 100858.

[8] Z. Sun, J. Wu, H. Yuan, J. Lan, Y. Yu, Y. Zhu, X. Yang, Self-healing polymer electrolyte for long-life and recyclable lithium-metal batteries, Mater. Today Energy 24 (2022) 100939.

[9] C. Fang, Y. Wang, W. Liu, R. Guo, G. Dang, Y. Zhang, H. Pei, Y. Li, S.S. Mao, S. Yu, J. Xie, Room temperature surface-engineering enabling stability of high-energy-density lithium batteries, Mater. Today Energy 17 (2020) 100415.

[10] X. Wang, G. Pawar, Y. Li, X. Ren, M. Zhang, B. Lu, A. Banerjee, P. Liu, E.J. Dufek, J.-G. Zhang, J. Xiao, J. Liu, Y.S. Meng, B. Liaw, Glassy Li metal anode for high-performance rechargeable Li batteries, Nat. Mater. 19 (2020) 1339−1345.

[11] S.L. Koch, B.J. Morgan, S. Passerini, G. Teobaldi, Density functional theory screening of gas-treatment strategies for stabilization of high energy-density lithium metal anodes, J. Power Sources 296 (2015) 150−161.

[12] J. Jiao, G. Lai, L. Zhao, J. Lu, Q. Li, X. Xu, Y. Jiang, Y.-B. He, C. Ouyang, F. Pan, H. Li, J. Zheng, Self-Healing mechanism of lithium in lithium metal, Adv. Sci. n/a (2022) 2105574.

[13] A. Jana, S.I. Woo, K.S.N. Vikrant, R.E. García, Electrochemomechanics of lithium dendrite growth, Energy Environ. Sci. 12 (2019) 3595−3607.

[14] M.W. Swift, Y. Qi, First-principles prediction of potentials and space-charge layers in all-solid-state batteries, Phys. Rev. Lett. 122 (2019) 167701.

[15] K. Leung, DFT modelling of explicit solid−solid interfaces in batteries: methods and challenges, Phys. Chem. Chem. Phys. 22 (2020) 10412−10425.

[16] C. Yuan, W. Lu, J. Xu, Unlocking the electrochemical−mechanical coupling behaviors of dendrite growth and crack propagation in all-solid-state batteries, Adv. Energy Mater. 11 (2021) 2101807.

[17] K. Tantratian, H. Yan, K. Ellwood, E.T. Harrison, L. Chen, Unraveling the Li penetration mechanism in polycrystalline solid electrolytes, Adv. Energy Mater. 11 (2021) 2003417.

[18] R. Huston, J.N. Butler, Standard potential of the lithium electrode in aqueous solutions, J. Phys. Chem. 72 (1968) 4263−4264.

[19] E. Santos, W. Schmickler, The crucial role of local excess charges in dendrite growth on lithium electrodes, Angew. Chem. Int. Ed. 60 (2021) 5876−5881.

[20] J.S. Chickos, Heat of sublimation data, NIST chemistry WebBook, NIST Standard Reference Database 69 (1998).

[21] W.R. Fawcett, Thermodynamic parameters for the solvation of monatomic ions in water, J. Phys. Chem. B 103 (1999) 11181−11185.

[22] J. Rumble, CRC Handbook of Chemistry and Physics, 102th ed.internet edition, CRC Press/Taylor & Francis, Boca Raton, FL, 2021.

[23] S. Trasatti, The absolute electrode potential: an explanatory note (Recommendations 1986), Pure Appl. Chem. 58 (1986) 955−966.

[24] F. Faglioni, B.V. Merinov, W.A. Goddard, Room-temperature lithium phases from density functional theory, J. Phys. Chem. C 120 (2016) 27104−27108.

[25] K. Leung, S.B. Rempe, O.A.v. Lilienfeld, Ab initio molecular dynamics calculations of ion hydration free energies, J. Chem. Phys. 130 (2009) 204507.

[26] E. BiÉmont, Y. Frémat, P. Quinet, Ionization potentials of atoms and ions from lithium to tin (Z= 50), Atomic Data Nucl. Data Tables 71 (1999) 117−146.

[27] E. Gileadi, The enigma of metal deposition, J. Electroanal. Chem. 660 (2011) 247−253.

[28] Y. Li, Y. Qi, Energy landscape of the charge transfer reaction at the complex Li/SEI/electrolyte interface, Energy Environ. Sci. 12 (2019) 1286−1295.

[29] Z. Wang, M. Li, C. Ruan, C. Liu, C. Zhang, C. Xu, K. Edström, M. Strømme, L. Nyholm, Conducting polymer paper-derived mesoporous 3D N-doped carbon current collectors for Na and Li metal anodes: a combined experimental and theoretical study, J. Phys. Chem. C 122 (2018) 23352−23363.

[30] M. Jäckle, A. Groß, Microscopic properties of lithium, sodium, and magnesium battery anode materials related to possible dendrite growth, J. Chem. Phys. 141 (2014) 174710.

[31] J. Zheng, M.S. Kim, Z. Tu, S. Choudhury, T. Tang, L.A. Archer, Regulating electrodeposition morphology of lithium: towards commercially relevant secondary Li metal batteries, Chem. Soc. Rev. 49 (2020) 2701−2750.

[32] M. Paunovic, M. Schlesinger, Fundamentals of Electrochemical Deposition, John Wiley & Sons, 2006.

[33] D. Pletcher, R. Greff, R. Peat, L. Peter, J. Robinson, Instrumental Methods in Electrochemistry, Elsevier, 2001.

[34] D. Rehnlund, C. Ihrfors, J. Maibach, L. Nyholm, Dendrite-free lithium electrode cycling via controlled nucleation in low LiPF6 concentration electrolytes, Mater. Today 21 (2018) 1010−1018.

[35] R. Zhang, X.-B. Cheng, C.-Z. Zhao, H.-J. Peng, J.-L. Shi, J.-Q. Huang, J. Wang, F. Wei, Q. Zhang, Conductive nanostructured scaffolds render low local current density to inhibit lithium dendrite growth, Adv. Mater. 28 (2016) 2155−2162.

[36] A. Pei, G. Zheng, F. Shi, Y. Li, Y. Cui, Nanoscale nucleation and growth of electrodeposited lithium metal, Nano Lett. 17 (2017) 1132−1139.

[37] S. Jin, Y. Jiang, H. Ji, Y. Yu, Advanced 3D current collectors for lithium-based batteries, Adv. Mater. 30 (2018) 1802014.

[38] D. Rehnlund, F. Lindgren, S. Böhme, T. Nordh, Y. Zou, J. Pettersson, U. Bexell, M. Boman, K. Edström, L. Nyholm, Lithium trapping in alloy forming electrodes and current collectors for lithium based batteries, Energy Environ. Sci. 10 (2017) 1350−1357.

[39] K.N. Wood, M. Noked, N.P. Dasgupta, Lithium metal anodes: toward an improved understanding of coupled morphological, electrochemical, and mechanical behavior, ACS Energy Lett. 2 (2017) 664−672.

[40] C. Fang, J. Li, M. Zhang, Y. Zhang, F. Yang, J.Z. Lee, M.-H. Lee, J. Alvarado, M.A. Schroeder, Y. Yang, B. Lu, N. Williams, M. Ceja, L. Yang, M. Cai, J. Gu, K. Xu, X. Wang, Y.S. Meng, Quantifying inactive lithium in lithium metal batteries, Nature 572 (2019) 511−515.

[41] C. Fang, B. Lu, G. Pawar, M. Zhang, D. Cheng, S. Chen, M. Ceja, J.-M. Doux, H. Musrock, M. Cai, B. Liaw, Y.S. Meng, Pressure-tailored lithium deposition and dissolution in lithium metal batteries, Nat. Energy 6 (2021) 987−994.

[42] J. Xiao, How lithium dendrites form in liquid batteries, Science 366 (2019) 426−427.

[43] L. Chen, H.W. Zhang, L.Y. Liang, Z. Liu, Y. Qi, P. Lu, J. Chen, L.-Q. Chen, Modulation of dendritic patterns during electrodeposition: a nonlinear phase-field model, J. Power Sources 300 (2015) 376−385.

[44] K.S. Exner, Constrained ab initio thermodynamics: transferring the concept of surface Pourbaix diagrams in electrocatalysis to electrode materials in lithium-ion batteries, Chemelectrochem 4 (2017) 3231−3237.

[45] K.S. Exner, Recent advancements towards closing the gap between electrocatalysis and battery science communities: the computational lithium electrode and activity−stability volcano plots, ChemSusChem 12 (2019) 2330−2344.

[46] Y. Liu, X. Xu, O.O. Kapitanova, P.V. Evdokimov, Z. Song, A. Matic, S. Xiong, Electro-chemo-mechanical modeling of artificial solid electrolyte interphase to enable uniform electrodeposition of lithium metal anodes, Adv. Energy Mater. 12 (2022) 2103589.

[47] X. Shen, R. Zhang, X. Chen, X.-B. Cheng, X. Li, Q. Zhang, The failure of solid electrolyte interphase on Li metal anode: structural uniformity or mechanical strength? Adv. Energy Mater. 10 (2020) 1903645.